

## **N-doped carbon quantum dots for 4-NP detection, anti-oxidant activity, and synthesis of $\text{Fe}_3\text{O}_4\text{CuO}@\text{CQD}$ as a catalyst for the reduction of 4-nitroaniline**

Namrata Priyadarshini Hota, Prakash Seenu, Nandhini Karthikeyan, Naveen Kumar, and

Sathiyanarayanan Kulathu Iyer\*

Department of Chemistry, School of Advanced Sciences, Vellore Institute of Technology, Vellore-632

014, India. \*E-mail: [sathiyanarayananank@vit.ac.in](mailto:sathiyanarayananank@vit.ac.in)

### **Table of Contents:**

1. Quantum Yield Measurement-----	<b>S1</b>
2. FT-IR analysis of Turmeric-derived CQDs -----	<b>S2</b>
3. FT-IR Spectra of Turmeric-derived CQDs -----	Figure <b>S1</b>
4. Comparison Table of different sensors for PA detection-----	Table <b>S1</b>
5. Comparison Table of quantum yield of different quantum dots -----	Table <b>S2</b>
6. Synthesis of $\text{Fe}_3\text{O}_4$ Nanoparticles-----	<b>S3</b>
7. Synthesis of CuO Nanoparticles-----	<b>S4</b>
8. Comparison table of $\text{Fe}_3\text{O}_4/\text{CuO}@\text{CQD}$ nanocomposite for Reduction of 4-NA-----	Table <b>S3</b>
9. Mechanism of the reduction of 4-Nitroaniline-----	<b>S5</b>

## **S1 Quantum Yield Measurement:**

Using quinine sulfate ( $\phi = 0.54$  in 0.1M H<sub>2</sub>SO<sub>4</sub>) as a standard reference, we determined the quantum yield of carbon dots. Using the following formula, the quantum yield was determined.

$$\Phi_{CQD} = \Phi_R \times \frac{I_{CQD}}{I_R} \times \frac{A_R}{A_{CQD}} \times \frac{n^2_{CQD}}{n^2_R}$$

In the equation above, CQD and R stand for the carbon dot and reference, respectively. "I" represents the integrated fluorescence intensity, "A" represents the absorbance value at the departing wavelength, and "n" denotes the solvent medium's refractive index (water has a refractive index of 1.33). Following the computation of each value, the quantum yield was **36.40%**.

## **S2 FT-IR analysis of Turmeric-derived CQDs**

The FTIR spectrum of NCQDs shows a broad band around 3344 cm<sup>-1</sup> corresponding to -OH/-NH stretching vibrations. However, this peak alone cannot be considered definitive evidence of nitrogen incorporation, as similar functional groups are also present in turmeric-derived CQDs. Nitrogen doping in carbon quantum dots predominantly alters the electronic structure and surface passivation rather than introducing distinct new functional groups detectable by FTIR. Therefore, the successful incorporation of nitrogen is primarily reflected in the enhanced photoluminescence intensity, higher quantum yield, and improved sensing performance of NCQDs compared to undoped CQDs.

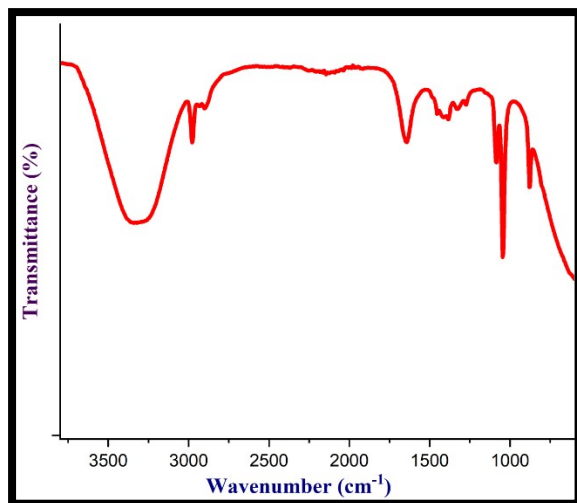


Figure S1 FT-IR Spectra of Turmeric-derived CQDs

**Table S1: Comparison Table of different quantum dots for PA detection:**

Sensing Probe for 4-NP	Linear range ( $\mu M$ )	LoD ( $nM$ )	Ref.
Citric acid and urea-based			[ <i>Journal of hazardous materials</i> 386 (2020): 121643]
Nitrogen-Doped Carbon Dots	2-100	200	
S, NCQD from citric acid and thiourea-aminophenol and dithioacetamide	0-85	37	[ <i>Spectrochimica Acta Part A: Molecular and Biomolecular Spectroscopy</i> 308 (2024): 123709]
NCQD from celery leaves and L-glutathione	0-0.35	26	[ <i>New Journal of Chemistry</i> 44, no. 4 (2020): 1500-1507.]

Giloy Stem based S, NCQD	0.5-6	380	[ <i>ACS omega</i> 10, no. 6 (2025): 5874-5885.]
<b>Nitrogen-doped from turmeric and L-arginine- based CQD</b>	<b>0-40</b>	<b>30</b>	<b>[This work]</b>

**Table S2 Comparison Table of quantum yield of different quantum dots**

No	Carbon sources	Quantum Yield (QY%)	References
1	Turmeric-based CQDs	~8.6	A. Prasannan, T. Imae, <i>Ind. Eng. Chem. Res.</i> , 2013, 52, 15673–15678
2	Orange peel CQDs	6.9	S. Zhu <i>et al.</i> , <i>Chem. Commun.</i> , 2012, 48, 4527–4529
3	Grass CQDs	7.5	Y. Liu <i>et al.</i> , <i>J. Mater. Chem.</i> , 2012, 22, 17402–17406
4	Green Tea leaves CQDs	9.0	S. Zhu <i>et al.</i> , <i>Chem. Commun.</i> , 2012, 48, 4527–4529
5	Garlic extract CQDs	10.5	H. Li <i>et al.</i> , <i>New J. Chem.</i> , 2015, 39, 707–712
6	<b>Turmeric and L-arginine-based CQDs</b>	<b>36.40</b>	<b>This work</b>

### S3. Synthesis of $\text{Fe}_3\text{O}_4$ Nanoparticles:

$\text{Fe}_3\text{O}_4$  nanoparticles were synthesized using NCQD, which served as both stabilizing and reducing agents. A 0.1 M  $\text{FeSO}_4 \cdot 7\text{H}_2\text{O}$  (2.79 g) solution was prepared in 100 ml of double-distilled water while stirring continuously. After adding 20 milliliters of NCQD to the solution, it was placed in an oil bath at 80°C. Next, 0.2 M of NaOH was added dropwise to keep the pH between 11 and 12, and the mixture was stirred for two hours. The mixture was found to be brown at first, but after NaOH was added, it turned black, signifying the creation of  $\text{Fe}_3\text{O}_4$  NPs. The mixture was centrifuged multiple times using acetone, ethanol, and water once it reached room temperature. After drying in an oven and being verified by several characterization methods, the  $\text{Fe}_3\text{O}_4$  NPs were utilized as a catalyst to create substituted imidazole scaffolds.

#### S4. Synthesis of CuO Nanoparticles:

The previously synthesized NCQD was used to create the CuO nanoparticles. A 100 ml round-bottom flask was used to initially dissolve 0.05 M of Cu (NO<sub>3</sub>)<sub>2</sub>. 2H<sub>2</sub>O in double-distilled water. Ten milliliters of the NCQD were then added to the copper nitrate solution, which turned light green following the complete dissolution. The reaction mixture was then maintained at 80°C. The pH was then brought to 12 by adding 0.5M of NaOH dropwise. Within five minutes, the solution's green hue turned to black, signifying the development of CuO nanoparticles. The reaction mixture was agitated for one and a half hours after that. To obtain the pure CuO nanoparticles, the reaction mixture was allowed to cool to ambient temperature and centrifuged multiple times using acetone, ethanol, and water.

**Table S3. Comparison table of Fe<sub>3</sub>O<sub>4</sub>/CuO@CQD nanocomposite for Reduction of 4-NA:**

Sl. No	Catalyst	Catalyst loading	Degradation time (min)	Reference
2	AuNPs	1 mL	9	[Nanoscale research letters 10 (2015): 1-8.]
3	Au–Pd bimetallic nanoparticles	0.5 mg	40	[Scripta materialia 54, no. 5 (2006): 909-914]
4	AgNPs	1 mL	480 sec	[Journal of Cluster Science 27 (2016): 285-298]
5	AgNPs/GAgNPs/GR-G3.0PAMAM nanocatalyst	10 mg	120 sec	[Journal of Molecular Catalysis A: Chemical 359 (2012): 88-96]
6	Fe <sub>3</sub> O <sub>4</sub> /CuO@CQD	2 mg	100 sec	<b>This work</b>

#### S5 Mechanism of the reduction of 4-Nitroaniline

The mechanism involves the following steps, and the plausible mechanism is given below. At first, 4-nitroaniline adsorbs via  $\pi$ – $\pi$  interactions with CQDs and coordination to metal oxide sites. Simultaneously, 4-nitroaniline starts to reduce with the adsorption of BH<sub>4</sub><sup>–</sup> ions on the Fe<sub>3</sub>O<sub>4</sub>/CuO@CQD surface. By acting as efficient electron mediators, CQDs facilitate quick electron transport from BH<sub>4</sub><sup>–</sup> to the nitro group through Fe<sub>3</sub>O<sub>4</sub> and CuO. In order to create p-

phenylenediamine, which subsequently desorbs and regenerates the catalyst surface, the nitro group is gradually reduced through nitroso and hydroxylamine intermediates.

